ChemBioChem

Combining Chemistry and Biology

Chemistry Europe

European Chemical Societies Publishing

Accepted Article

Title: Design and Evaluation of Artificial Hybrid Photoredox Biocatalysts

Authors: Timothy Daniel Schwochert, Cole Cruz, John W. Watters, Evan W. Reynolds, David A. Nicewicz, and Eric Brustad

To be cited as: *ChemBioChem* 10.1002/cbic.202000362

Link to VoR: https://doi.org/10.1002/cbic.202000362

WILEY-VCH

10.1002/cbic.202000362

WILEY-VCH

FULL PAPER

Design and Evaluation of Artificial Hybrid Photoredox Biocatalysts

Timothy D. Schwochert[a], Cole L. Cruz[a], John W. Watters[a], Evan W. Reynolds[a], David A. Nicewicz[a], Eric M. Brustad[a],[b]

[a] T. D. Schwochert, Dr. C. L. Cruz, J. W. Watters, Prof. D. A. Nicewicz, Prof. E. M. Brustad
Department of Chemistry
University of North Carolina at Chapel Hill
125 South Road CB 3290, Chapel Hill, NC 27599 (USA)

[b] Current address:
Illumina, Inc.
5200 Illumina Way, San Diego, CA 82130
E-mail: ebrustad@illumina.com

Supporting information for this article is given via a link at the end of the document.

Abstract: A pair of 9-mesityl-10-phenyl acridinium (Mes-Acr$^+$) photoredox catalysts were synthesized with an iodoacetamide handle for cysteine bioconjugation. Covalently tethering of the synthetic Mes-Acr$^+$ cofactors with a small panel of thermostable protein scaffolds resulted in twelve newly reported artificial enzymes. The unique chemical and structural environment of the protein hosts had a measurable effect on the photophysical properties and photocatalytic activity of the cofactors. The constructed Mes-Acr$^+$ hybrid enzymes were found to be active photoinduced electron transfer catalysts, controllably oxidizing a variety of aryl sulphides when irradiated with visible light and possessed activities that correlated with the photophysical characterization data. Catalytic performance was found to be dependent on multiple factors including the Mes-Acr$^+$ cofactor, the protein scaffold, the location of cofactor immobilization, and the substrate. This work provides a framework toward adapting synthetic photoredox catalysts into artificial cofactors and includes important considerations for future bioengineering efforts.

Introduction

Nature supplements the reactivity of enzymes through the recruitment of small molecule cofactors that impart chemical functionality not available to native amino acids. Inspired by this resourcefulness, protein engineers have expanded the breadth of enzyme catalysis by designing hybrid systems that combine the unique reactivity of synthetic catalysts - as artificial cofactors - with the control and structural complexity endowed by biomolecular scaffolds.[1-3] The selection of artificial cofactors for bioengineering applications has historically been guided by the field of small molecule homogenous catalysis, most notably centered on transition metal catalysis due to the rich and diverse chemistries enabled by these complexes.[4,5] Importantly, the properties of the protein-bound metal catalysts can be tuned by proximal and distal amino acids to enhance turnover, stereoselectivity, stability, and activity in water.[6,7] Furthermore, this marriage of chemical ingenuity and protein engineering has led to the development of artificial metalloenzymes capable of performing a number of new-to-nature chemical transformations.[8,9]

Based on the success of artificial metalloenzyme engineering, there is growing interest in expanding the scope of artificial cofactors to encompass other catalytic modalities.[10,11] For example, photoredox catalysis has shown increased application for chemical synthesis due to its broad utility in bond activation via mechanisms that are often orthogonal or complementary to traditional transition metal chemistry.[12,13] Photoredox transformations operate through photoinduced electron transfer (PET) events, which facilitate the generation of highly reactive intermediates at ambient temperature bypassing thermal barriers and permitting access to unique reactivity patterns. Intriguingly, nature already employs a number of photoexcitable chromophores that initiate light-driven single electron redox pathways in order to drive and regulate a variety of biological processes. Select examples include the use of chlorophyll and carotenoids in photosynthesis[14] and flavins in reversible light-activated signal transduction pathways.[15] However, the functions of most photoexcitable proteins in biology are highly specific, rendering their broad-scoped application as synthetic photoredox catalysts quite challenging.

Despite the limited synthetic utility of natural light-harvesting proteins, Hyster and coworkers have recently identified promiscuous photoredox activity in non-light activated enzymes that bind chromophoric cofactors, including nicotinamide-[16] and flavin-dependent oxidoreductases.[17] This work takes advantage of the excited-state synthetic potential of the natural cofactors in conjunction with the enzyme's substrate binding cavities, which enables substrate access, binding, and orientation in proximity to the chromophore. Although, due to the limited structural and electronic diversity of photoactivatable cofactors in nature, the synthetic repertoire accessible to these systems is inherently restricted.[18] On the other hand, there is a wealth of diversity among reported synthetic photoredox catalysts which can be tuned to have a broad range of redox potentials and wavelengths for excitation.[12,13] We believe the adaptation of these synthetic photoredox catalysts as artificial cofactors will provide a general and systematic approach to expand light-driven biocatalysis with the potential to generate diverse new-to-nature chemical reactivities.

There have been a number of reports describing the immobilization of photocatalysts onto protein scaffolds to serve as mediators for controlling the redox state of natural cofactors.[19,20] However, the direct use of photoredox catalysts to carry out biocatalytic transformations on small molecules is underexplored. Lewis and colleagues reported the first example of a hybrid enzyme appended to a non-natural photoredox cofactor.[21] In their design, a cyclooctyne-modified Fukuzumi catalyst was immobilized within an engineered cavity of prolyl peptidase via click reaction to an unnatural amino acid side

chain. The hybrid photo-enzyme showed improved photostability for the cofactor due to immobilization within the hydrophobic interior of the protein cavity. However, diminished photocatalytic oxygenase activity was observed compared to the free cofactor. Beyond this report, there are no other examples of the construction of artificial cofactors as a means to directly install PET activity into enzymes for small molecule synthesis.

Results and Discussion

We set out with the goal of designing a set of novel artificial photoredox cofactors which could be linked to a variety of protein scaffolds. In recent years, the organic dye 9-mesityl-10-phenyl acirindium (Mes-Acr$^+$) has emerged as a powerful excited state oxidant, catalyzing a diverse array of photoredox transformations when irradiated with visible light.[13,22-23] Due to its utility, multiple generations of the organic Mes-Acr$^+$ catalysts with different properties have emerged such as **1a** and **2a** (Figure 1A).[24,25] The more recently developed **2a** is decorated with a pair of methyl groups on the acridinium core which have been shown to improve catalyst stability and performance in select applications. Based on these precedents, we hypothesized Mes-Acr$^+$ could serve well as an artificial cofactor and would hopefully retain its powerful light-driven catalytic properties in a protein environment. Two Mes-Acr$^+$ cofactor derivatives (**1b** & **2b**) were synthesized with an iodoacetamide handle for covalent anchoring to a host protein via cysteine alkylation (Figure 1A, see supplemental methods).

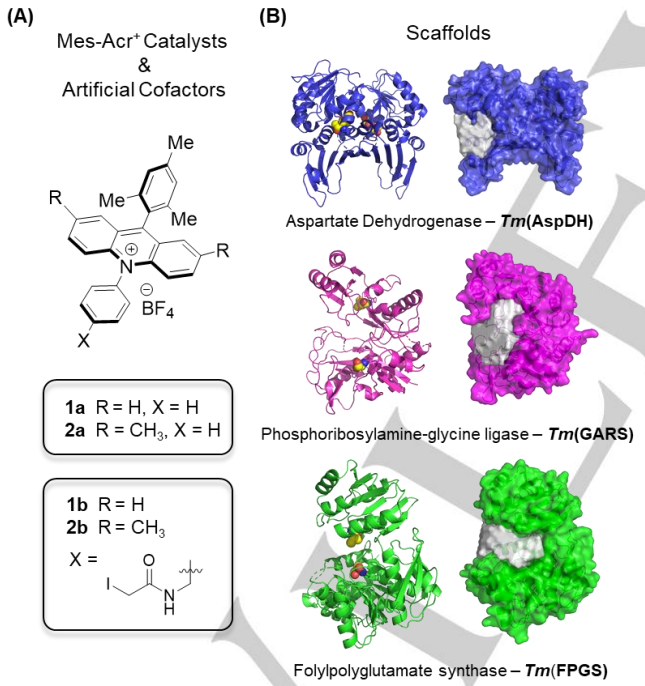

Figure 1. (A) Mes-Acr$^+$ catalysts and artificial cofactors synthesized with an iodoacetamide handle for covalent attachment to the protein scaffold. **(B)** Biomolecules from *T. Maritima* selected for artificial cofactor immobilization. Engineered cysteines in scaffold cavities for covalent attachment of cofactors are shown as spheres (left). Protein concavities for artificial cofactor active sites are shown in grey (right). PDB id's for scaffolds, AspDH: (1J5P), GARS: (1VKZ), FPGS: (1O5Z).

In order to select protein hosts for these novel artificial cofactors, we scanned the Protein Data Base for biomolecular scaffolds with concavities in their tertiary structure that would sufficiently accommodate the Mes-Acr$^+$ cofactors (see supplemental methods). We chose to explore multiple protein scaffolds because it has been shown that the identity of scaffold can have a substantial effect on the properties of the synthetic cofactors.[6,26] Furthermore, varying the attachment residue within the same scaffold can also vary the behavior of a bound catalyst.[27] By screening multiple scaffolds for the Mes-Acr$^+$ cofactors and a pair of cysteine conjugation residues for each scaffold, we surmised this would increase our chances to observe context dependent interactions between the host and cofactor. We restricted our scaffold search to proteins from thermophilic organisms, as these proteins generally possess high thermostability and provide promising initial platforms for further mutation and design. We selected three protein scaffolds, all from the thermophile *Thermotoga Maritima (Tm),* which include an aspartate dehydrogenase (AspDH), phosphoribosylamine-glycine ligase (GARS), and folylpolyglutamate synthase (FPGS). All three proteins possess large cavities to accomodate the photocatalyst (Figure 1b). Following inspection of the amino acid residues within the cavity interiors, we chose two different residue positions in all three scaffolds for cysteine mutagenesis to covalently attach **1b** and **2b** (Figure 1B). In the preparation and design of host proteins, it was important to note that *Tm*(AspDH) and *Tm*(FPGS) both contain one or more endogenous cysteines, none of which participate in disulfide bonds. Accordingly, these native cysteines were mutated to a valine or serine prevent heterogeneous cofactor attachment. Ultimately, covalent attachment of these engineered scaffolds with **1b** and **2b** through cysteine alkylation (see supplemental methods) resulted in a small library of twelve artificial enzymes. Bioconjugation of artificial cofactors was confirmed via high resolution mass spectrometry (Table S1, Figure S1 and S2).

With the new artificial Mes-Acr$^+$ conjugates in hand, we first examined their photophysical properties in buffered solution. We believe this initial characterization to be an important first step in the analysis of photoactive cofactors as the ground and excited state behavior of the catalyst ultimately govern the catalyst's photoredox activity. UV/Vis experiments surveying for alterations in the ground state revealed no significant changes in the absorbance profile of **1b** and **2b** when bound to the protein scaffolds with the exception of moderate red shifting of 1 - 2 nm for both cofactors (Figure S3). In all experiments, protein-bound cofactors were compared with the parent **1a** and **2a** Mes-Acr$^+$ catalysts in lieu of the iodoacetamide derivatives because heavy atoms such as iodine can influence photochemical and photophysical properties.[28]

The steady state fluorescence and excited state lifetimes (τ_f) for the enzyme library were then analyzed as these metrics can have an effect on excited state electron transfer. Reductions in quantum yield of fluorescence (Φ_f) or τ_f in the absence of substrate can indicate static and dynamic quenching respectively, both inefficient pathways drawing away from the desired electron transfer iniating catalysis. With respect to Φ_f (Table S2), one protein scaffold, AspDH, increased fluorescence emission of **1a** when irradiated with 425 nm light. For both cofactor attachment positions (T223C & S226C) of the scaffold, Φ_f was increased 2-2.5 fold (Figure 2). Both *Tm*(GARS) and *Tm*(FPGS) caused a notable reduction (2 – 3 fold) in Φ_f for **1**, indicating some degree of scaffold-induced quenching. *Tm*(AspDH) is unique in that it does not contain tryptophan residues, an aromatic side chain that can induce quenching on protein-conjugated fluorophores that may contribute to the descreased fluorescence observed in *Tm*(GARS) and *Tm*(FPGS). These results show that the structural environment of the protein catavity can impose distinct photophysical properities on the artificial cofactor.

(A)

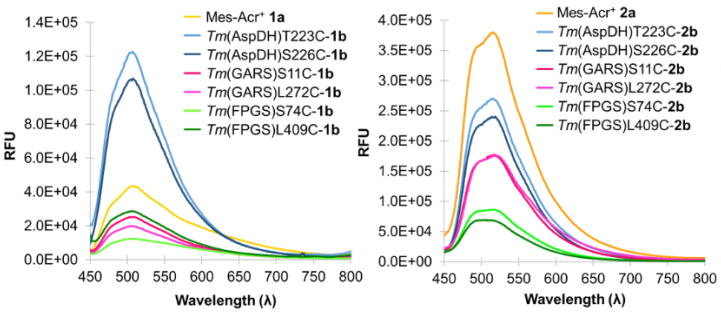

(B)

Catalyst	$\frac{\Phi_f}{\Phi_{f\,1a}}$	measured τ_f (ns)
Mes-Acr⁺ **1a**	1.00	7.19
Tm(AspDH)T223C-**1b**	2.45	8.01
Tm(AspDH)S226C-**1b**	1.93	8.38
Tm(GARS)S11C-**1b**	0.59	8.27
Tm(GARS)L272C-**1b**	0.41	8.18
Tm(FPGS)S74C-**1b**	0.30	8.33
Tm(FPGS)L409C-**1b**	0.60	8.99

Catalyst	$\frac{\Phi_f}{\Phi_{f\,2a}}$	measured τ_f (ns)
Mes-Acr⁺ **2a**	1.00	12.04
Tm(AspDH)T223C-**2b**	0.68	10.45
Tm(AspDH)S226C-**2b**	0.59	11.86
Tm(GARS)S11C-**2b**	0.46	9.08
Tm(GARS)L272C-**2b**	0.49	9.86
Tm(FPGS)S74C-**2b**	0.23	9.45
Tm(FPGS)L409C-**2b**	0.18	8.94

Figure 2. (A) Steady state fluorescence emission spectra of unbound and protein bound Mes-Acr⁺ catalysts when irradiated with 425 nm light in relative fluorescence units. **(B)** Tables showing ratio of unbound Mes-Acr⁺ Φ_f to protein scaffold bound **1b** or **2b** and fluorescence lifetimes (in ns) Mes-Acr⁺ catalysts measured at 510 nm by time-correlated single photon counting, $\lambda_{excitation}$ = 444 nm. Emission spectra and lifetime data were both collected at 20µM Mes-Acr⁺ derivatives in 25 mM Tris buffer pH 7.5 with 10% acetonitrile under the same instrument parameters.

Interestingly, the trend of increasing emission did not carry over for cofactor **2b** as all protein scaffolds and all cofactor attachment positions resulted in attenuated Φ_f (Figure 2A). However, in the case of **2b** and consistent with catalyst **1b**, *Tm*(AspDH) showed the least perturbation of catalyst flourescence. Unbound Mes-Acr⁺ **2a** was shown to be a much more emissive species than **1a** and may be less sensitive to quenching effects of the buffered aqueous environment (Figure 2A). The *Tm*(AspDH) scaffold still permitted the most emissive form of protein-conjugated **2b** with ~60-70% Φ_f when compared to the unbound cofactor followed by *Tm*(GARS) and then *Tm*(FPGS).

To further characterize the excited state of our constructed enzymes, τ_f was measured using time-correlated single photon counting experiments (Figure 2B and Figures S4). The fluorescence plots were fit to multi-exponential decays, highlighting the complicated excited-state behavior of these species in the aqueous buffers.[21,29] A small increase of 1-2 nanoseconds (ns) in τ_f was measured across all scaffolds for **1b** indicating relaxation-pathways may be weakly mitigated when bound to the tested scaffolds. Conversely, when **2b** is attached to the protein scaffolds τ_f was measured to be lower across a range of 0.2 to 3 ns in comparison to **2a** with *Tm*(AspDH) showing a slight reduction in lifetime.

The suite of 12 hybrid enzymes were then evaluated as photoredox catalysts in the oxidation of aryl thioethers to sulfoxides (see supplemental methods and Figure S5). Sulfoxidation reactions are generally performed through two electron chemical oxidation requiring stoichiometric amounts of a sacrificial oxidant and run the risk of overoxidation to the sulfone.[30] Due to this, photocatalytic methods using O_2 to trap radical intermediates have been explored as alternatives and offer greener and potentially more controllable processes.[31]

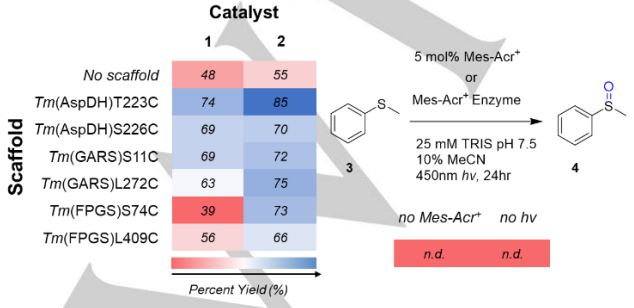

Figure 3. Screen of Mes-Acr⁺ catalysts and hybrid enzymes in the photoinduced oxidation of thioansiole with yields shown in the heat map above. n.d. = not detected.

To test if the excited state of our artificial enzymes could controllably oxidize aryl thioethers with atmospheric O_2, the enzymes were irradiated with 450 nm LEDs in the presence of a model substrate, thioanisole (Figure 3).

Nearly all of the scaffolds and variants increased yield of the desired methyl phenyl sulfoxide for both artificial cofactors **1b** and **2b** when compared to the unbound catalysts. The Mes-Acr⁺ catalyst **2** also outperformed **1** in all reactions, whether free or bound to a protein scaffold. *Tm*(AspDH)T223C-**2b** was an efficient sulfoxidation catalyst and yielded 85% of the desired sulfoxide product compared to a 55 % yield observed with the free cofactor, **2a**. Both these results correlated well with the photophysical characterization data as **2a** and the *Tm*(AspDH) conjugates consistently provided the most desirable excited state properties for PET. In addition, no over oxidation of the sulfoxide to the sulfone was observed by GCMS analysis (Figure S2).

Control experiments showed that both light and the presence of catalyst were necessary for product formation (Figure 3). To further probe the mechanism of the reaction, a Stern-Volmer analysis was performed on the *Tm*(AspDH)-**2b** variants with thioanisole as a quencher.The excited state was quenched in a linear manner across a range of thioanisole concentrations for free and bound cofactors, indicative of a mechanism proceeding through PET (Figure S6).

Based on these initial results, a small set of 10 aryl thioethers were then analyzed as sulfoxidation substrates for the two variants of *Tm*(AspDH) conjugated to **2b**, the more reactive cofactor (Figure 4). Electron withdrawing and donating groups on the arenes were tolerated as well as ethyl and benzyl aryl thioethers. No general trends were observed with respect to the protein variant and free catalyst. In most cases, comparable yield or a modest increase in yield were observed for the protein bound catalyst. Decreased yield was observed for chloro- and nitro-substituted thioethers **9** and **11**. Some notable improvements in product turnover were observed in specific cases. Notably, in the case of napthyl-substituted substrate **7**, the free cofactor provide only 24 % yield for the sulfoxide product, whereas, *Tm*(AspDH)T223C-**2b** increased the reaction yield to 81 %. However, *Tm*(AspDH)T226C-**2b**, only increased product yield to 39 %. Chiral analysis of the sulfoxide products revealed that none of the tested scaffolds resulted in observable enantiomeric enrichment (Figure S3). Taken together, these results show that the hybrid Mes-Acr⁺ enzymes displayed a range of efficiencies in mediating photoinduced sulfoxidation and the activity is not only substrate dependent but also varies across the cofactors and scaffolds tested.

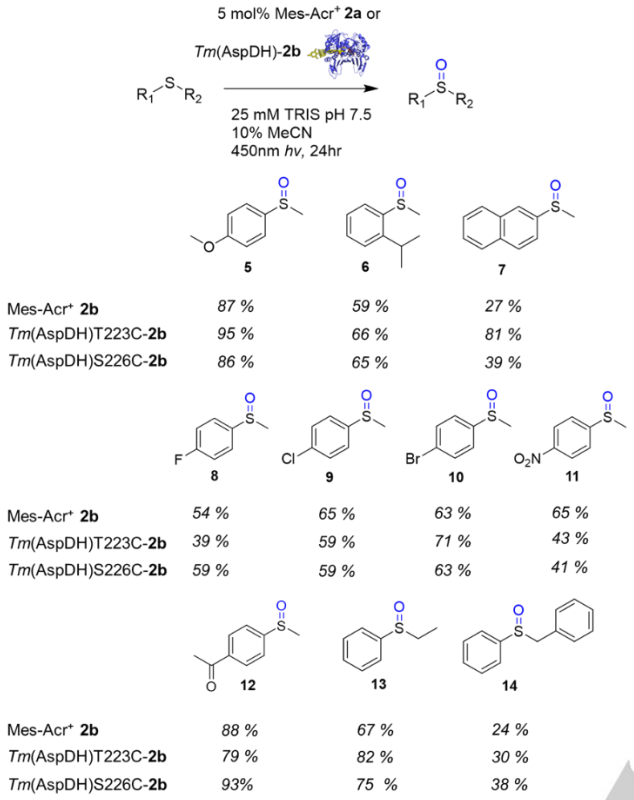

Figure 4. Sulfoxidation of aryl-substitued thioethers catalyzed by Mes-Acr$^+$ **2a** and best scaffold hit *Tm*(AspDH) with **2b**.

Conclusion

In summary, we report the preparation, characterization, and application of twelve novel artificial photoredox enzymes. Two derivatives of the organic photoredox catalyst, 9-mesityl-10-phenyl acirindium (Mes-Acr$^+$), were synthesized and covalently tethered to three thermostable protein scaffolds at two different anchoring sites each. The photophysical properties of each of the bound Mes-Acr$^+$ catalysts were analyzed and compared alongside the free cofactor in solution. It was found that the identity of the protein scaffold can have a measurable effect on the quantum yield of fluorescence and excited state lifetime of the chromophore, both important properties for applications in photoredox catalysis. Reaction screening of the Mes-Acr$^+$-modified protein scaffolds revealed all are active photoenzymes, but the performance of these catalysts towards light-driven sulfoxidation is dependent on multiple factors including the artificial cofactor, the protein scaffold, the location of cofactor immobilization, and the reaction substrate. It is likely that a single protein scaffold will not be sufficient to serve as a general platform for catalysis and that there is significant benefit in generating a library of hybrid protein scaffolds for reaction screening. The field of engineering artificial photoredox cofactors is still very young and we anticipate that the general design strategy presented herein as well as the specific Mes-Acr$^+$ cofactors and protein scaffolds in this study will be informative for future artificial biocatalysis developments.

Acknowledgements

This work was supported by a National Science Foundation (NSF) Career Award (CHE-1552718). This research made use of instrumentation funded by the UNC EFRC: Center for Solar Fuels, an Energy Frontier Research Center supported by the U.S. Department of Energy, Office of Science, Office of Basic Energy Sciences, under award number DE-SC0001011.

Keywords: Artificial Cofactors • Biocatalysis • Artificial Enzyme • Photoredox Catalysis • Sulfoxidation

[1] M. E. Wilson, G. M. Whitesides, *J. Am. Chem. Soc.* **1978**, *100*, 306–307.
[2] S. Abe, J. Niemeyer, M. Abe, Y. Takezawa, T. Ueno, T. Hikage, G. Erker, Y. Watanabe, *J. Am. Chem. Soc.* **2008**, *130*, 10512–10514.
[3] I. S. Hassan, A. N. Ta, M. W. Danneman, N. Semakul, M. Burns, C. H. Basch, V. N. Dippon, B. R. McNaughton, T. Rovis, *J. Am. Chem. Soc.* **2019**, *141*, 4815–4819.
[4] F. Schwizer, Y. Okamoto, T. Heinisch, Y. Gu, M. M. Pellizzoni, V. Lebrun, R. Reuter, V. Köhler, J. C. Lewis, T. R. Ward, *Chem. Rev.* **2018**, *118*, 142–231.
[5] H. J. Davis, T. R. Ward, *ACS Cent. Sci.* **2019**, *5*, 1120–1136.
[6] H. M. Key, P. Dydio, D. S. Clark, J. F. Hartwig, *Nature* **2016**, *534*, 534–537.
[7] G. Sreenilayam, E. J. Moore, V. Steck, R. Fasan, *ACS Catal.* **2017**, *7*, 7629–7633.
[8] H. Yang, A. M. Swartz, H. J. Park, P. Srivastava, K. Ellis-Guardiola, D. M. Upp, G. Lee, K. Belsare, Y. Gu, C. Zhang, et al., *Nature Chemistry* **2018**, *10*, 318–324.
[9] T. K. Hyster, L. Knörr, T. R. Ward, T. Rovis, *Science* **2012**, *338*, 500–503.
[10] C. J. Seel, T. Gulder, *ChemBioChem* **2019**, *20*, 1871–1897.
[11] L. Zhang, J. Yuan, Y. Xu, Y.-H. P. Zhang, X. Qian, *Chem. Commun.* **2016**, *52*, 6471–6474.
[12] M. H. Shaw, J. Twilton, D. W. C. MacMillan, *J. Org. Chem.* **2016**, *81*, 6898–6926.
[13] N. A. Romero, D. A. Nicewicz, *Chem. Rev.* **2016**, *116*, 10075–10166.
[14] H. A. Frank, R. J. Cogdell, *Photochemistry and Photobiology* **1996**, *63*, 257–264.
[15] J. M. Christie, *Annu. Rev. Plant Biol.* **2007**, *58*, 21–45.
[16] M. A. Emmanuel, N. R. Greenberg, D. G. Oblinsky, T. K. Hyster, *Nature* **2016**, *540*, 414–417.
[17] B. A. Sandoval, A. J. Meichan, T. K. Hyster, *J. Am. Chem. Soc.* **2017**, *139*, 11313–11316.
[18] L. Schmermund, V. Jurkaš, F. F. Özgen, G. D. Barone, H. C. Büchsenschütz, C. K. Winkler, S. Schmidt, R. Kourist, W. Kroutil, *ACS Catal.* **2019**, *9*, 4115–4144.
[19] N.-H. Tran, N. Huynh, T. Bui, Y. Nguyen, P. Huynh, M. E. Cooper, L. E. Cheruzel, *Chem. Commun.* **2011**, *47*, 11936–11938.
[20] V. Sosa, M. Melkie, C. Sulca, J. Li, L. Tang, J. Li, J. Faris, B. Foley, T. Banh, M. Kato, et al., *ACS Catal.* **2018**, *8*, 2225–2229.
[21] Y. Gu, K. Ellis-Guardiola, P. Srivastava, J. C. Lewis, *ChemBioChem* **2015**, *16*, 1880–1883.
[22] P. D. Morse, D. A. Nicewicz, *Chem. Sci.* **2014**, *6*, 270–274.
[23] L. Wang, F. Wu, J. Chen, D. A. Nicewicz, Y. Huang, *Angewandte Chemie International Edition* **2017**, *56*, 6896–6900.
[24] K. Ohkubo, K. Mizushima, R. Iwata, K. Souma, N. Suzuki, S. Fukuzumi, *Chem. Commun.* **2010**, *46*, 601–603.
[25] D. J. Wilger, J.-M. M. Grandjean, T. R. Lammert, D. A. Nicewicz, *Nature Chemistry* **2014**, *6*, 720–726.
[26] H. M. Key, P. Dydio, Z. Liu, J. Y.-E. Rha, A. Nazarenko, V. Seyedkazemi, D. S. Clark, J. F. Hartwig, *ACS Cent. Sci.* **2017**, *3*, 302–308.
[27] R. R. Davies, H. Kuang, D. Qi, A. Mazhary, E. Mayaan, M. D. Distefano, *Bioorganic & Medicinal Chemistry Letters* **1999**, *9*, 79–84.
[28] Lakowicz, J. R. Principles of Fluorescence Spectroscopy, 3rd ed.; Springer: New York, **2006**.
[29] G. Jones, D. Yan, J. Hu, J. Wan, B. Xia, V. I. Vullev, *J. Phys. Chem. B* **2007**, *111*, 6921–6929.

[30] S. Velusamy, A. V. Kumar, R. Saini, T. Punniyamurthy, *Tetrahedron Letters* **2005**, *46*, 3819–3822.
[31] X. Gu, X. Li, Y. Chai, Q. Yang, P. Li, Y. Yao, *Green Chem.* **2013**, *15*, 357–361.

10.1002/cbic.202000362

WILEY-VCH

Entry for the Table of Contents

Insert graphic for Table of Contents here. ((Please ensure your graphic is in **one** of following formats))

((max. width: 11.5 cm; max. height: 2.5 cm))

Please delete this box prior to submission

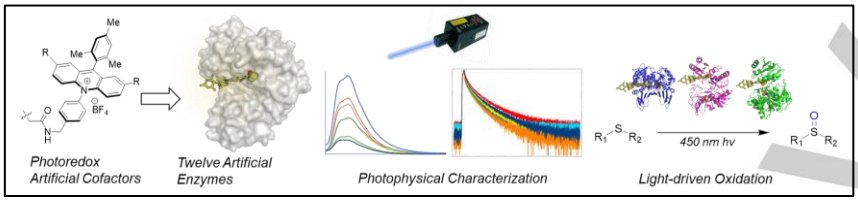

Shining Light on Enzymes. Here we report the design and evaluation of two artificial organic photoredox cofactors in the context of multiple protein scaffold hosts. The ground and excited-state properties of the free and scaffold-bound cofactors were measured, as the photophysical properties govern the photocatalytic activity. The engineered artificial enzymes were found to be active excited-state oxidants, acting on a range of aryl sulfides.

((The Table of Contents text should give readers a short preview of the main theme of the research and results included in the paper to attract their attention into reading the paper in full. The Table of Contents text **should be different from the abstract** and should be no more than 450 characters including spaces.))